ARTICLE IN PRESS

Materials Today: Proceedings xxx (xxxx) xxx

Contents lists available at ScienceDirect

Materials Today: Proceedings

journal homepage: www.elsevier.com/locate/matpr

In-situ thermal monitoring informed modeling and simulation of process temperature during vat photopolymerization additive manufacturing

Heyang Zhang, Xiayun Zhao *

ZXY Intelligent Precision - Advanced Manufacturing (ZIP-AM) Laboratory, Department of Mechanical Engineering & Materials Science, University of Pittsburgh, Pittsburgh, PA 15261, United States

ARTICLE INFO

Article history:
Available online xxxx

Keywords:
Additive manufacturing
Vat photopolymerization
Thermal monitoring
Thermal simulation

ABSTRACT

Vat photopolymerization (VPP) 3D printing is an additive manufacturing (AM) process in which liquid photopolymer is selectively cured using light-activated polymerization to create a desired 3D part. Since the curing reaction is exothermic, the process of printing will generate heat and affect the resin rheology, curing kinetics and printed part properties. It is important to know the temperature of the printing process, especially at the resin-part interface where the temperature distribution could indicate the anisotropic degree of conversion and residual stress among other temperature-related properties. However, it is difficult to measure the print interface in a desired non-contact approach due to the limited viewability and accessibility of the curing zone being sandwiched between solid build head and liquid resin. Existing work based on simulation has limited accuracy due to model assumptions and unknown/uncertain parameters. In this work, we demonstrate a framework of VPP-AM process temperature measurement methods that combine in-situ thermal monitoring and finite element-based model simulation. An in-situ temperature monitoring protocol is established to calibrate or obtain the thermal properties of VPP material system as well as measure the reachable surface temperature (e.g., resin chamber substrate, build head). These in-situ measurements are input to a physics-based model and simulation is conducted to estimate the desired temperature profile of the resin-part interface. To validate the developed thermal monitoring-informed simulation approach, we use a characterized bottom-up thermal imaging setup to monitor single-layer VPP printing, and our experiment result shows a good agreement between the simulation and direct measurement results.

1. Introduction

Vat photopolymerization (VPP) 3D printing is an additive manufacturing (AM) process in which liquid photopolymers is selectively cured using light-activated polymerization section by section to create a desired 3D part [1]. PAM mainly uses ultraviolet (UV) light to initiate the photopolymerization of the raw liquid material. One way the light is delivered is through digital light processing (DLP), in which LED light is masked using digital micromirror devices. This allows the resin to be cured one layer at a time, as opposed to one voxel at a time as in stereolithography (SLA). The photopolymerization reaction in the printing process is exothermic and could cause thermal gradients and thus printing issues. In general, we can expect variations in the degree of conversion (DoC) of printed parts since the reaction rate of polymerization is a function of temperature that is varying during the printing process. Especially in the presence of high temperature and large thermal gradient, which are usually associated with large-format printing, the printed parts could undergo severe deformation and degradation due to issues such as residual stress and thermal cracking [2]. Besides, the process temperature has proven to be influential on the resin viscosity and curing performance [3].

Overall, the temperature during VPP, especially DLP based VPP that prints one cross-section at a time, is subject to change due to the polymerization reaction and in turn can significantly affect the curing kinetics, resin rheology, process stability, and part properties. Information of the DLP based VPP process temperature is needed for optimal process control but difficult to obtain due to the lack of direct measurement techniques. Contact thermal

* Corresponding author.
E-mail address: xiayun.zhao@pitt.edu (X. Zhao).

https://doi.org/10.1016/j.matpr.2022.09.027
2214-7853/

Please cite this article as: H. Zhang and X. Zhao, In-situ thermal monitoring informed modeling and simulation of process temperature during vat photopolymerization additive manufacturing, Materials Today: Proceedings, https://doi.org/10.1016/j.matpr.2022.09.027

measurements are infeasible since it need be either embedded into the cured part or block the projected light to the active print region. Infrared measurements will not work since the print interface is not IR-visible due to being sandwiched between the printed part and the resin vat. As such, the limited viewability or accessibility of the curing region necessitates a method of indirectly measuring the temperature. In particular, the resin-part interface temperature profile directly affects the photopolymerization process dynamics and cured part properties. However, it is difficult to directly measure without probing into the curing zone.

There are minimal works in literature to characterize the temperature of VPP printing processes such as stereolithography (SLA) [4,5]. Recent literature work has shown that the photopolymerization mechanism within SLA can be accurately simulated to predict properties such as geometric warping and temperature. However, such models are restrained with in one control volume (voxel) [5], or to a single layer in 2 dimension [4], and cannot capture real process deviations since they solely rely on some inadequate physics models with simplifying assumptions and unknown/uncertain parameters.

In this work, to fill the gaps above, we develop an in-situ thermal monitoring informed model simulation method that can infer the resin-part interface temperature by combining in-situ thermography from outside the resin chamber with a heat transfer model and finite element (FE) simulation. This model will approximate the geometry of a 3-D print, building upon the models that are constraint by the dimensions. A commercial simulation software - COMSOL Multiphysics® - is used to implement the model simulation for predicting the temperature at the active curing region. The developed model will serve as a baseline for a more comprehensive Multiphysics model that can consider the chemical reactions and dependent variables. The framework of VPP-AM process temperature estimation methods will provide a technical guidance for monitoring VPP processes with good accuracy and offer insights about the process kinetics and material evolution to predict part properties.

2. System and methods

2.1. VPP system

Fig. 1 shows the schematics of a typical DLP VPP printer, also the one used in this work. The DLP image is projected through the bottom of the resin chamber, in this case, through a polydimethylsiloxane (PDMS) bottom. The PDMS substrate permits the oxygen to diffuse into the liquid resin, generating an inhibition zone to isolate the print parts from the substrate [6]. To allow in-situ thermal imaging of the print area with an infrared (IR) thermal camera from the top, we custom a build head (print head) using IR transparent material. The print starts with the build head inserting into the resin. After one layer is cured, the print head moves up by a specified layer thickness, and the void will be filled by the surrounding uncured resin and then a new layer is cured. This layer-by-layer process is repeated until the target 3D part is fabricated.

2.2. In-situ thermal monitoring

We develop an in-situ temperature monitoring protocol to calibrate and obtain the thermal properties of VPP material system as well as measure the reachable surface temperature (e.g., resin chamber substrate, build head). These in-situ measurements are input to a physics-based model and simulation is conducted to estimate the desired temperature profile of the resin-part interface.

The printed part is observed using a thermal camera (FLIR ThermaCAM S40) at two positions. One is on-axis above the print through the print head. A 1-inch ZnSe broadband window (Thorlabs WG71050) is fashioned into a printhead as it is transparent in the IR wavelength used by the thermal camera. The other observed position is off-axis under the print vat at a 20-degree angle from the surface of the vat. The emissivity of the surface observed is calibrated using a thermal couple at the appropriate angles of contact. Position A, from Fig. 2, is measured to have an emissivity of 0.85, and Position B, from Fig. 2, had an emissivity of 0.98.

The purpose of Position A setup is to collect data for better understanding and simulation of the polymerization process as well as provide a validation step for the exothermic model of the polymerization chemistry. A thermal camera placed at Position B, however, would be the sensor used ultimately to validate and provide feedback for the simulation parameters in the future.

2.3. Physics model and finite element based simulation

We can describe this system using a basic transient thermal equation with a complicated heat generation term, shown in Equation (1).

$$\frac{\partial^2 T_{resin}}{\partial r^2} + \frac{1}{r}\left(\frac{\partial T_{resin}}{\partial r}\right) + \frac{\partial^2 T_{resin}}{\partial z^2} + \frac{q_{active}}{k} = \frac{1}{\alpha}\frac{\partial T_{resin}}{\partial t} \quad (1)$$

Herein, instead of solving this explicitly, COMSOL is used to solve the thermal system. For faster processing, an axisymmetric assumption is made as the printed part is a cylinder. Four parts of geometry is assumed. The PDMS vat layer at the bottom, labeled A; a layer of bis-EMA on top of the vat, labeled B; a subset of the bis-EMA, i.e., the thickness of the print layer being the "active

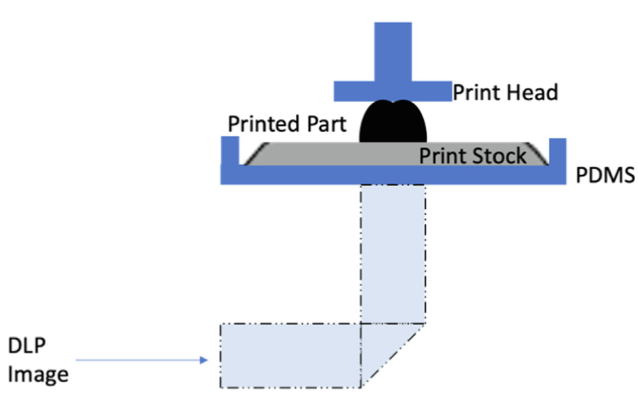

Fig. 1. Representation of DLP VPP Printer.

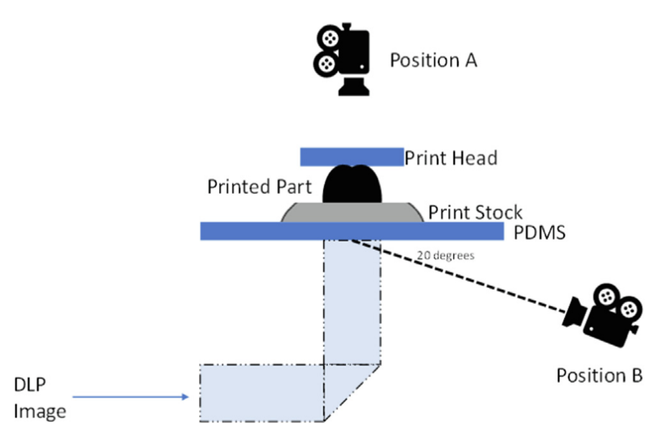

Fig. 2. Position of the thermal camera.

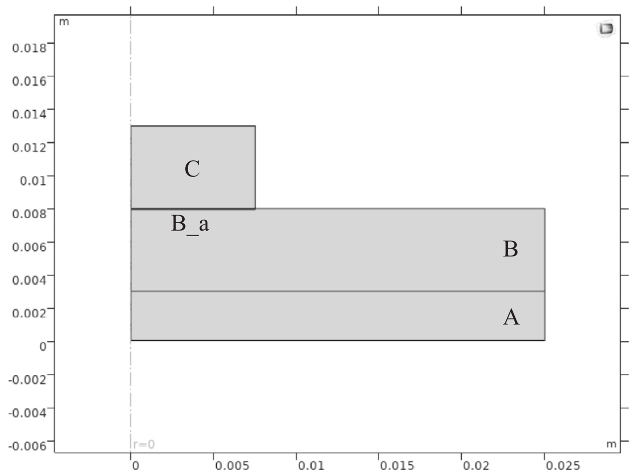

Fig. 3. Geometry used in COMSOL.

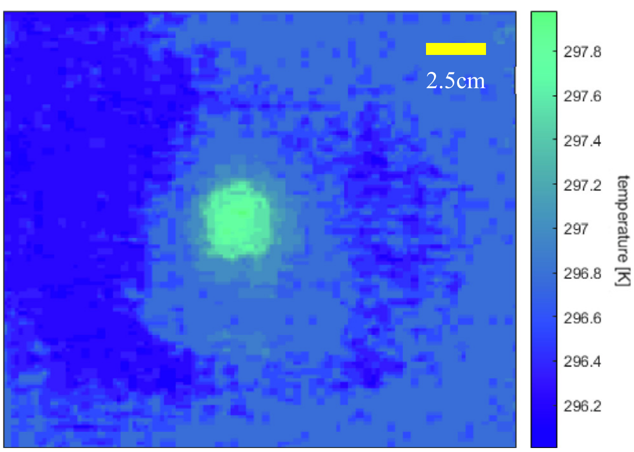

Fig. 4. A representative thermography of the printed part taken from the top with the camera looking down through the build head (Position A).

region", labeled B_a; and a printed part bis-EMA with varied density to emulate the increasing layers of bis-EMA, labeled C. The printed part, C, has a density that is a step function which starts at 0, and increases by increments such that the total mass of C is equivalent to the mass of the printed layers. The geometry is shown in Fig. 3.

A thermal insulation boundary condition is used in all outward facing surfaces, and a pre-set temperature is set at the active region using the thermal gradient measured from Fig. 4(a) and (b). Assumptions are made for the thermal properties of both the resin and PDMS to be invariant relative to temperature.

3. Experimental design and material

3.1. Experiment design

In this work, as a demo case, simple cylinders are printed using our in-house DLP printer. A circle with 10 mm in diameter is used as the projected image. The light power received by the print area is measured to be 3.34mW at the print stage (without PDMS), and 2.81mW through the PDMS substrate, using an optical power meter (THORLABS PM400 with 10 mm diameter sensor). The nominal printing process is set up with a one second LED (460 nm) on time and 1 s of LED off time for each layer. In practice, it takes about 3.6 s per layer. The layer thickness is set to be 0.05 mm. 100 layers are printed for each sample with a target thickness of 5 mm. There are signs of overcuring, which causes the parts to be around 15 mm in diameter and 6 mm thick instead of the desired 10 mm in diameter and 5 mm thick. Nevertheless, the replications of printing result in consistent part sizes throughout the experiments. The overcuring is mainly due to the non-optimal process setting, which is outside the scope of this work.

Table 1
Estimated thermal properties of bis-EMA.

Property	Value	Source
Resin conductivity	0.2 W/mK	[8]
Resin density	965 kg/m^3	[9]
Resin diffusivity	1×10^{-7} m^2/s	[10]

Table 2
Thermal properties of PDMS.

Property	Value	Source
PDMS conductivity	0.15 W/mK	[11]
PDMS density	965 kg/m^3	[11]
PDMS heat capacity	1.46 kJ/kg K	[11]

3.2. Materials

The resin recipe is based on the works of de Beer et al [7]. Bisphenol A ethoxylate diacrylate (Bis-EMA, and BPAEDA in de Beer's work) is used as the resin with camphorquinone (CQ) as the photo-initiator, and ethyl 4-(dimethylamino)benzoate (EDAB) as the co-initiator. Bis-EMA was selected due to many outside factors, namely stock availability at the time. The material system allows us to cure the resin using blue light at the wavelength of 460 nm.

Although there's little literature on the thermal parameters of bis-EMA – i.e., the thermal conductivity, heat capacity, and thermal diffusivity – we can find values of similar resins, summarized in Table 1. Further investigation will be required for exact values but is unreasonable at this stage of work.

The resin vat is created using PDMS. This is used to create a dead zone at the bottom of the vat. The thermal properties of PDMS are better documented and summarized in Table 2.

4. Result of In-Situ thermography measurements

2-D measurements of temperature are made through the in-situ thermography Position A during all the experimental VPP prints as shown in Fig. 4 The measured maximum temperature is used represent the transient response, as shown in Fig. 5(a) and (b).

From Position A, we can measure the maximum temperature of the printed part. We can observe from Fig. 4(b) a linear increase in temperature before the effects of diffusion takes over the active region's temperature. From the measurement, we can observe a thermal rate of 0.1 degrees per second (0.1 K/s) in the first 4 layers printed.

5. Simulation result and experimental validation

Implementing the model and simulation method as introduced in Section 2, in COMSOL, a pre-set temperature at 0.1 K/s is set at the active region using the thermal rate measured from Position A setup (see Fig. 5), we can estimate the resin-part interface temperature distribution. We simulate the 2D temperature profile at

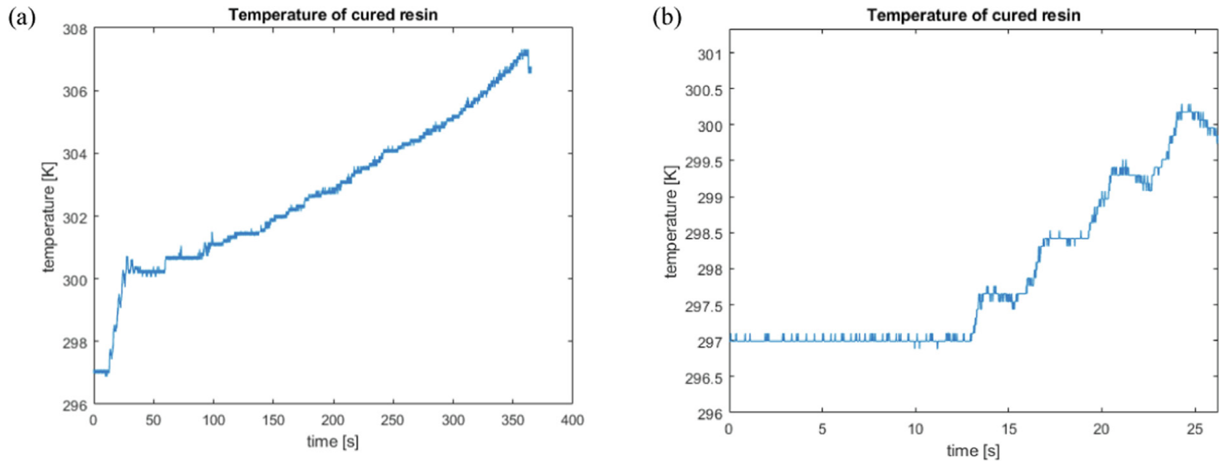

Fig. 5. (a) Maximum temperature of resin from Position A (b) zoomed in.

the resin-part interface and validate the results by examining the single point of maximum temperature as well as the 2D distribution.

5.1. Measuring the maximum temperature of curing region

One key temperature metric of interest is the maximum temperature in the curing region, since it indicates how significant the temperature effect could be and help estimate the worst thermal damage scenario. The max temperature occurs at the center of curing region between the print part and vat substrate. We assume that the curing region center and the vat substrate center coincide considering their distance is on the order of microns and thus negligible. This assumption eases the extraction of the temperature from the thermography which is used to provide a ground truth measurement for validating the simulation result. In the simulation of maximum temperature, a virtual probe is placed at the bottom of the vat at r = 0 to measure the max temperature at the

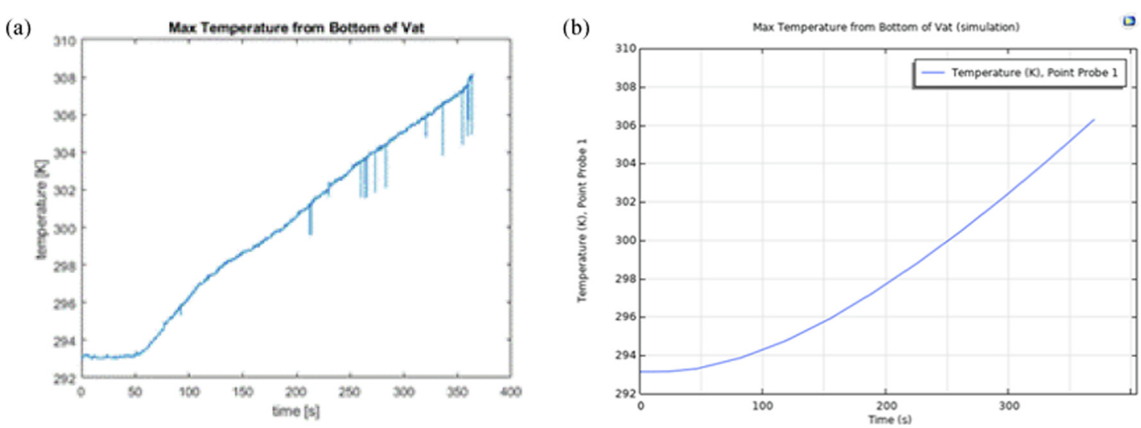

Fig. 6. (a) Actual (thermography) and (b) Predicted (model) max temperature at the bottom center of the vat.

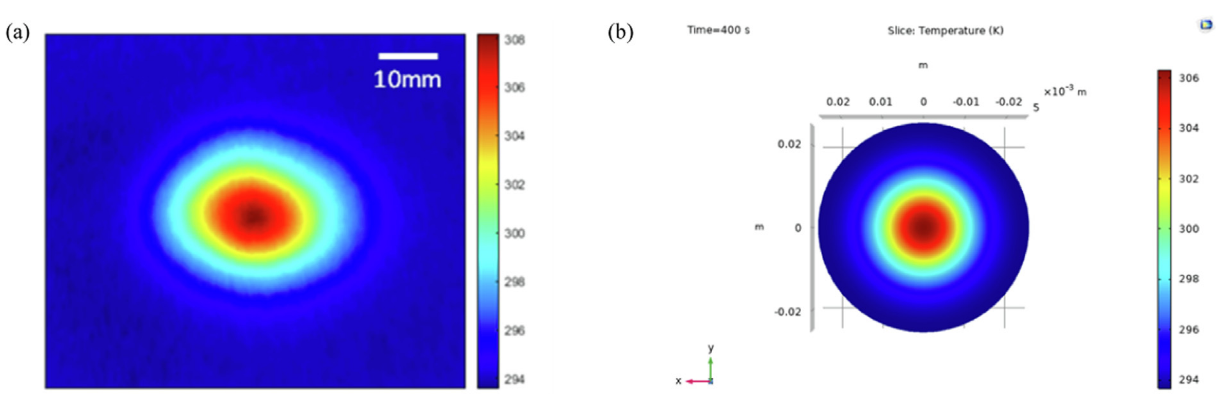

Fig. 7. (a) Measured and (b) Predicted temperature distribution of the curing region observed at the bottom of the vat while printing the last layer.

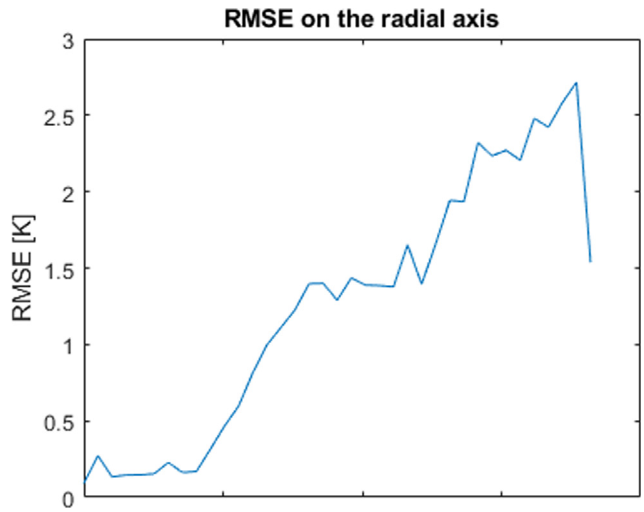

Fig. 8. RMSE of the predicted temperature of the bottom of the vat on the r-axis.

bottom of the vat, same position as the value taken from the thermography.

In validation experiment, by using the thermal camera to view from the bottom side of the vat (Position B as shown in Fig. 1), a circular temperature profile is observed as the heat from the exothermic polymerization reaction is diffused to the vat substrate (PDMS). There is zero temperature change for the first 60 s, and after the delay a constant temperature change rate is observed. The delay is due to the diffusivity of heat from the heat source to the measured surface and is a function of mainly the diffusivity of the resin and PDMS. We can notice, from Fig. 6 (a) and (b) that the simulation is able to show the delay of temperature change until around 60 s, as well as the temperature change from 293 K to 307 K through the entirety of the print.

5.2. Measuring the 2D temperature distribution of curing region

After comparing the single-point measurement of the maximum temperature (Fig. 6), we further investigate the simulation of 2D temperature distribution of the curing region. As we mentioned earlier, the 2D temperature field at the resin-part interface directly affects the kinetics rates across the print area and thus induce anisotropic curing. A snapshot of the temperature profile at the end of the print is presented in Figs. 7(a) and 6(b) for the thermal camera measurement and the simulation prediction, respectively. The thermal camera measure profile is not a perfect circle due to the perspective transformation errors.

Further analysis of the accuracy of the prediction is done by comparing the 2D temperature predicted to what is observed. An average of root mean square error (RMSE) difference of the temperature is done for every 10 s with the data points taken radially from the maximum temperature – which we assumed to be the center of the circle outwards. This is shown in Fig. 8. We can see that the predicted temperature is within a deviation of 2–3 degrees Kelvin for most cases.

6. Conclusion and further work

The developed in-situ monitoring informed model simulation method allows for taking surrounding temperatures that are more easily or directly measurable to infer the temperature profile across the curing area (resin-part interface). It mitigates the demanding in-situ thermal monitoring challenges, as we can place the thermal camera or thermocouple probes outside of the print area and approximate the temperature distribution in the print area.

This work lays down a strong foundation for the simulation of thermal diffusivity within VPP 3D printing. Further expansion of the simulation, with experiments to measure the thermal parameters of the material can increase the accuracy of the prediction. The next steps in terms of the simulation are to add the chemical kinetics and to better model the exothermic energy source. In the long term, a control system is to be created. The input being the printing parameters such as voxel light intensity, light on and off time, etc. to control the temperature in the active region. The thermal camera placed in Position B to measure the signal for feedback control.

Data availability

Data will be made available on request.

Declaration of Competing Interest

The authors declare the following financial interests/personal relationships which may be considered as potential competing interests: [Zhao Xiayun reports financial support was provided by NSF.]

Acknowledgements

This material is based upon work supported by the National Science Foundation under Grant No. CMMI-2134447. Any opinions, findings, and conclusions or recommendations expressed in this publication are those of the authors and do not necessarily reflect the views of the National Science Foundation. The authors would like to thank Professor Minking K. Chyu and Professor Nikhil Bajaj for their generous sharing of their infrared thermal cameras. This work also received great help and support from the authors' research team at the University of Pittsburgh, including: 1) Dr. Chaitanya Krishna P Vallabh for his help on the system development and suggestions; 2) graduate student Yue Zhang for her help with the material formulation and model simulation; and 3) undergraduate students (Shukai Wang, Haiwei Shi, and Anthony Berardelli) for their help in the experiment.

References

[1] ISO/ASTM, Additive manufacturing - General principles - Fundamentals and vocabulary. 2021. 52900:2021.
[2] D.A. Walker, J.L. Hedrick, C.A. Mirkin, Rapid, large-volume, thermally controlled 3D printing using a mobile liquid interface, Science 366 (6463) (2019) 360–364.
[3] X. Li, B. Xie, J. Jin, Y. Chai, Y. Chen, 3D Printing Temporary Crown and Bridge by Temperature Controlled Mask Image Projection Stereolithography, Procedia Manuf. 26 (2018) 1023–1033.
[4] K. Gao, B.L.J. Ingenhut, A.P.A. Van De Ven, F.O. Valega Mackenzie, A.T. ten Cate, Multiphysics modelling of photo-polymerization in stereolithography printing process and validation, in: COMSOL Conference. Lausanne, 2018.
[5] Y. Tang, Stereloithography Cure Process Modeling, School of Chemical & Biomolecular Engineering, Georgia Institute of Technology, 2005.
[6] J.R. Tumbleston, D. Shirvanyants, N. Ermoshkin, R. Janusziewicz, A.R. Johnson, D. Kelly, K. Chen, R. Pinschmidt, J.P. Rolland, A. Ermoshkin, E.T. Samulski, J.M. DeSimone, Continuous liquid interface production of 3D objects, Science 347 (6228) (2015) 1349–1352.
[7] Martin P. de Beer, H.L. Van Der Laan, Megan A. Cole, Riley J. Whelan, Mark A. Burns, TImothy F. Scott, Rapid, continuous additive manufactutring by volumetric polymerization inhibition patterning, Sci. Adv. 5 (2019).
[8] H. Oh et al., Enhancement of thermal conductivity of polymethyl methacrylate-coated graphene/epoxy composites using admicerllar polymerization with different ionic surfactants, Compos. A Appl. Sci. Manuf. 116 (2019) 206–215.
[9] Sigma-Aldrich, Bisphenol A ethoxylate diacrylate, in 64401-02-1.
[10] L. Silaghi-Dumitrescu, D. Dadarlat, M. Streza, T. Buruiana, D. Prodan, I. Hodisan, C. Prejmerean, Preparation of a new type of giomers and their thermal characterization by photopyroelectric calorimetry, J. Therm. Anal. Calorim. 118 (2) (2014) 623–630.
[11] J.E. Mark, Polymer Data Handbook, 2nd ed., 2009.